Journal of Chemical Health Risks

www.jchr.org

JCHR (2025) 15(3), 531-535| ISSN:2251-6727

Green synthesis and characterization of silver nanoparticle using *M.indica* and their anticancer activity against MCF-7

Saritha E[1*], Nivetha L[2], Mohanapriya B[3] and Vidyasri R[4]

[1,2]*Assistant Professor, Department of Biotechnology, PSG College of Arts & Science, Coimbatore-14, Tamil Nadu, India.*
[3]*Assistant Professor, Department of Biotechnology, Rathinam College of Arts & Science, Coimbatore- 21, Tamil Nadu, India.*
[4]*M.Sc Biotechnology, Department of Biotechnology, PSG College of Arts & Science, Coimbatore-14, Tamil Nadu, India*.
*Corresponding Author & Email: Dr. Saritha E & sarithasenthikumar@gmail.com

(Received: 16 March 2025 Revised:20 April 2025 Accepted: 01 May 2025)

KEYWORDS

AgNPs, *M. indica*, FTIR, FESEM and MCF-7.

ABSTRACT:

This work provides a safe, affordable and eco-friendly method for synthesizing silver nanoparticles (AgNPs) from leaves of *Mangifera indica*. The noticeable shift in colour from pale yellow to reddish-brown signifies a fast synthesis of AgNP. Validation of AgNPs was confirmed by a UV-Visible spectrum, FTIR, and DLS analysis. X-ray diffraction confirms the crystalline nature of AgNPs, and FESEM images show spherical, agglomerated nanoparticles. EDX analysis confirms metallic silver with elemental constituents of 50.03% silver and 49.97% oxygen, affirming successful silver ion reduction, that indicates good efficacy of *M. indica* leaf extract as a capping agent. AgNPs exhibited good inhibition zone against *E. coli*, *Streptococcus sp*, and *Staphylococcus sp* (15 mm, 13 mm & 14 mm). AgNPs indicating potent cytotoxicity on MCF-7 breast cancer cells, with a significant 14% reduction in cell viability at 250 µl.

1. Introduction

Greenly synthesised silver nanoparticles, or AgNPs, have a lot of applications in engineering, bioenergy, medicine, and bioremediation, among other areas. Their shape, size, optical and electrical properties, catalytic activity, and high surface area-to-volume ratio are among the attributes that drive their uses [1, 2]. Green nanotechnology provides an eco-friendly approach to synthesis functional nanoparticles such as iron, silver, and gold using plants, algae, and microorganisms. Plant-mediated green synthesis utilizes natural compounds like phenols, flavonoids, and alkaloids as reducing and stabilizing agents [3]. *M. indica* have phytochemicals like polyphenols, terpenoids, vitamins, and amino acids with various biological activities. These activities include antioxidant, antidiabetic, anti-inflammatory, antimicrobial, and anticancer properties.

2. Objectives

This research focuses on synthesizing AgNPs from *Mangifera indica*, investigating their physical and chemical characteristics, examining their antibacterial and anticancer effects.

3. Methods

Preparation of *Mangifera indica* aqueous extract

Fresh *M. indica* leaves were collected from Pattanam, Coimbatore, and taxonomic authentication was done at the Botanical Survey of India, Coimbatore, India (No: BSI/ SRC/ 5/ 23/ 2022/ Tech/ 144). The fresh leaves were washed with running tap water and shade dried. The aqueous leaf extract of *M. indica* was prepared [4].

Biosynthesis of AgNPs

Silver nanoparticles (AgNPs) were produced by mixing 10 mL of the filtrate with 90 mL of a 1 mM silver nitrate ($AgNO_3$) solution, and the mixture was kept in the dark for 24 h at room temperature to promote the reduction of silver ions. The successful synthesis of AgNPs was verified through UV-visible spectroscopy, which showed distinct absorption peaks characteristic of the nanoparticles [5].

Characterization of AgNPs

UV-Vis spectral analysis was performed with the Shimadzu UV-1700 UV-Visible spectrophotometer, which has a resolution of 1 nm and operates within the range of 200 to 800 nm. The functional groups in the

Journal of Chemical Health Risks
www.jchr.org
JCHR (2025) 15(3), 531-535| ISSN:2251-6727

silver nanoparticles (NPs) derived from *M. indica* were analyzed using the FTIR-Shimadzu IR Affinity Model 1S, a double-beam spectrometer with a wavenumber range of 4000 cm^{-1} to 400 cm^{-1} & a resolution of $10cm^{-1}$. Dynamic light scattering was conducted using Malvern Instrument to determine the average size and zeta potential of the AgNPs. The crystalline structure of the synthesized AgNPs was verified through X-ray diffraction. The structural morphology of the biosynthesized AgNPs was examined using field emission scanning electron microscopy (Zeiss FESEM SIGMA VP 03-04 model). Additionally, energy-dispersive X-ray spectroscopy (EDX) was utilized to analyze the elemental composition of the *M. indica* AgNPs.

***In Vitro* Susceptibility Test**

The antibacterial activity of AgNPs against human pathogens, which include Gram-positive bacteria (such as *Bacillus sp.*, *Staphylococcus aureus*, and *Streptococcus sp*.) and Gram-negative bacteria (like *Escherichia coli* and *Serratia sp*.), was assessed using the agar-well diffusion technique. The pathogenic strains were spread on Mueller-Hinton agar using a sterile cotton swab. The wells were loaded with 40 µl and 50 µl of *M. indica* AgNPs, with tetracycline as a control. The zone of inhibition was observed after 24 h of incubation at 37°C.

***In vitro* cytotoxicity assay**

AgNPs from *M. indica* were evaluated on MCF-7 cells using the MTT assay. The IC_{50} was determined by plotting concentration (µg/mL) against cytotoxicity (%). Cell imaging was carried out to determine cytotoxicity and cell viability through inverted phase-contrast microscopy.

4. Results and Discussion

Biosynthesis of AgNPs

The aqueous leaf extract of *M. indica* interacts with $AgNO_3$, resulting in color changes from light yellow to reddish brown, then to dark brownish-black, and finally to grey over the course of 24, 48, and 72 h, respectively. This indicates the production of silver nanoparticles (Figure 1a & b). The conversion of Ag^+ ions to Ag^0 nanoparticles is facilitated by functional groups such as O-H and =C-H found in various parts of the plant, including the bark, peel, callus, leaves, flowers, fruits, stem seeds, and rhizomes[6]. These findings were aligned with [5].

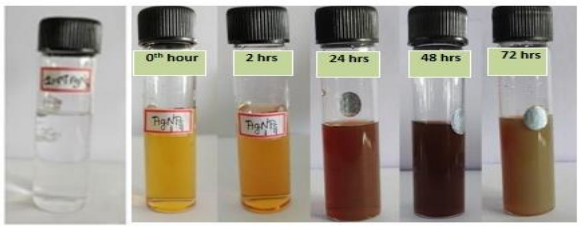

Figure 1: Synthesis of *M. indica* AgNPs
a) Control -1mM $AgNO_3$
b) Sample -1mM $AgNO_3$ + aqueous extract

Characterisation of AgNPs

The presence of silver nanoparticles (AgNPs) was confirmed by a broad peak at 457 nm, with the peak's widening indicating polydispersity due to variations in size, shape, and aggregation (Figure 2). AgNPs are typically exhibit a UV–Visible absorption between 400–500 nm attributed to surface plasmon resonance [7]. This SPR absorption peak is a result of the free electrons found in noble metals such as silver and gold [8].

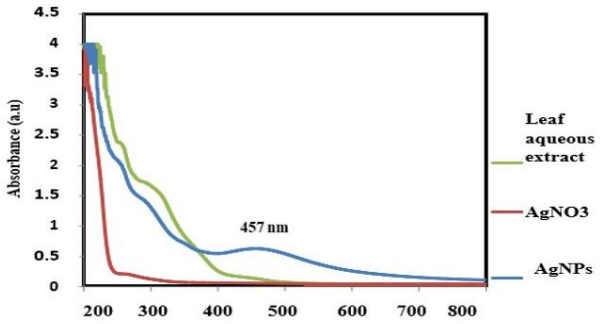

Figure 2: UV-Visible absorption spectrum of AgNPs from *M. indica*

Fourier Transform Infrared Spectrometer (FTIR)

The FTIR analysis showed that the prominent absorption bands at 1699.29 cm^{-1}, 1537.27 cm^{-1}, and 682.80 cm^{-1} corresponded to the stretching vibrations of C=O in conjugated aldehydes, N–O in nitro compounds, and C–Br in halo compounds, respectively. Additionally, the distinct band at 3595.31 cm^{-1} was attributed to the O–H stretching characteristic of alcohol (Figure 3). This study revealed presence of diverse functional groups on the nanoparticle surface suggesting, stability through bimolecular capping *via* electrostatic interactions that also responsible for silver ion reduction [9] investigated the above similar findings.

Journal of Chemical Health Risks
www.jchr.org
JCHR (2025) 15(3), 531-535| ISSN:2251-6727

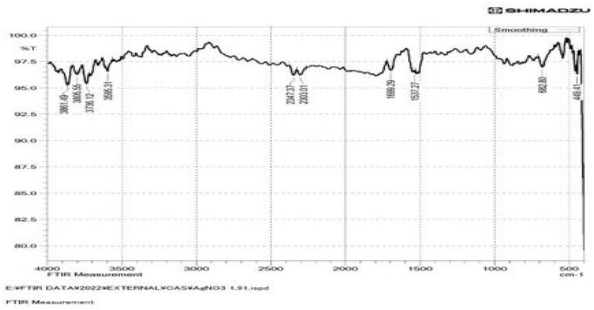

Figure 3: FTIR spectrum of AgNPs

DLS

DLS was used to analyse the average size, charge and stability of the biosynthesized silver nanoparticles. The results showed an average particle size of 63.88 nm with a PDI of 0.280 (Figure 4). The zeta potential of −16.4 mV indicates strong surface charges of the capping materials in stabilizing the AgNPs. Particles with a zeta potential higher than + 30 mV and lower than – 30 mV are indicative of stable NPs [3]. The higher zeta potential charges confirmed the long-term stability and repulsion force of the nanoparticles. The electrostatic repulsive forces between the nanoparticles upon being negatively charged may prevent aggregation, which thereby increases the stability of AgNPs [10].

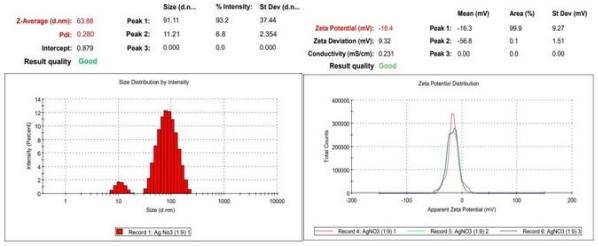

Figure 4: DLS-Based Size and Zeta Potential Analysis of AgNPs

X -Ray Diffraction

The crystalline nature of silver nanoparticles was identified by XRD diffraction analysis (Figure 5). The 2θ diffraction peaks observed at 38.78°, 44.14°, 64.67° and 78.30° corresponds to (111), (200), (220) and (311) planes, respectively. Silver typically exhibits a face-centred cubic (FCC) structure. The characteristic peaks for silver in an XRD pattern correspond to specific planes of the crystal lattice (e.g., (111), (200), (220) and (311). The same related finding was reported by [11].

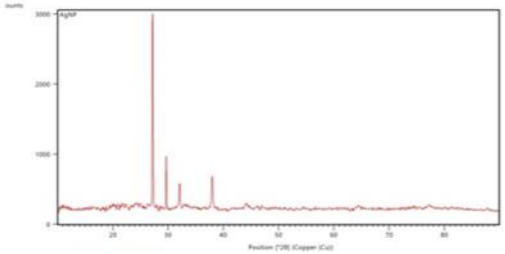

Figure 5: Crystalline Structure of Biogenic AgNPs by XRD

Field Emission Scanning Electron Microscopy (FESEM)

Field Emission Scanning Electron Microscopy (FESEM) is an advanced high-resolution imaging technique used to study the surface morphology, size, and distribution of silver nanoparticles. Two different magnification levels, 250,000x and 350,000x, were employed to analyse the topography and shape of the crystalline C-Ag nanoparticles. FESEM revealed agglomerated, spherical-shaped C-Ag NPs with a size of approximately 100 nm (Figure 6).

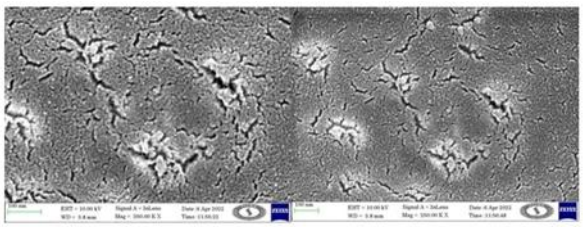

Figure 6: Topographical Characterization of AgNPs using FESEM

Energy Dispersive X-Ray (EDX)

The EDX spectrum shows a strong signal at 3 keV, confirming the presence of silver. The elemental composition of the nanoparticles was 50.03% silver and 49.97% oxygen (Figure 7), indicating that the *M. indica* leaf extract served as a capping agent on the AgNPs. Similar results were reported [9].

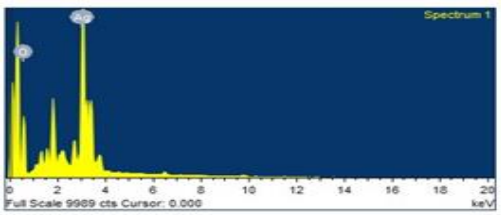

Figure 7: Elemental Composition Analysis of AgNPs Using EDX

Journal of Chemical Health Risks

www.jchr.org

JCHR (2025) 15(3), 531-535| ISSN:2251-6727

Antimicrobial Susceptibility Profiling of *M. indica* AgNPs

The AgNP (50 µL) showed the strongest antibacterial effects, resulting in inhibition zones of 15 mm for *E. coli*, 13 mm for *Streptococcus sp.*, and 14 mm for *Staphylococcus sp* (Figure 8) In contrast, the lowest antibacterial activity was observed at 40 µL, with inhibition zones of 9 mm for *Bacillus sp*. and 7 mm for *Serratia sp*. Antibacterial efficacy is influenced by nanoparticle concentration, bacterial species, and the enchanced reactivity of small particles, which generate more H_2O_2, induce oxidative stress, and cause apoptosis, leading to enhanced bactericidal effects [12].

Figure 8: Antibacterial Susceptibility profiling of *M.indica* AgNPs

Anti-neoplastic Potential of *M. indica* AgNPs on MCF-7

AgNPs exhibited a dose-dependent cytotoxic effect on the MCF-7 breast cancer cell line. At a concentration of 250 µL, cell viability dropped to 14% (Figure 9). Cell viability significantly decreasing as the concentration increases. The IC_{50} was found to be 28.9 µL, and complete cell death occurred at concentrations of 200 µL and 250 µL. The AgNPs derived from *M.indica* have potent cytotoxic effects on MCF-7, aligning with earlier research [13].

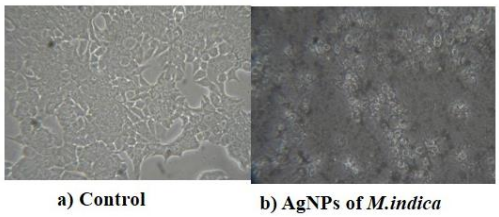

Figure 9: Anti-neoplastic Potential of *M. indica* AgNPs on MCF-7

Conclusion

This study successfully synthesized silver nanoparticles (AgNPs) using *M. indica* leaf extract, evidenced by a color change over 72 h. The nanoparticles were characterized by UV-Vis, FTIR, DLS, XRD, FESEM, and EDX, confirming their stability, crystalline nature, and spherical shape. The AgNPs exhibited strong antibacterial activity, particularly at 50 µL, and exhibited a dose-dependent cytotoxic effect on the MCF-7 breast cancer cell line, with complete cell death at higher concentrations. The findings highlight the significant antibacterial and anticancer potential of *M.indica*-derived AgNPs, supporting their potential use in biomedical applications.

Acknowledgement

The authors express their sincere gratitude to the Management and the Principal of PSG College of Arts & Science, Coimbatore, for their generous support and provision of necessary facilities to conduct this research. Additionally, we gratefully acknowledge the Department of Science and Technology (DST), New Delhi, for their financial assistance through the FIST grant, which was instrumental in completing this work.

Conflict of interest

The authors declare that there is no competing interest.

References

1. Jain A, Ahmad F, Gola D, Malik A, Chauhan N, Dey P, Tyagi PK, 2020a. Multi dye degradation and antibacterial potential of papaya leaf derived silver nanoparticles. *Environ Nanotechnol Monit Manag*, 14, 100337.
2. Alarjani KM, Huessien D, Rasheed RA, Kalaiyarasi M, 2022. Green synthesis of silver nanoparticles by *Pisum sativum* L. (pea) pod against multidrug resistant foodborne pathogens. *J King Saud Univ Sci*, 34(3), 101897.
3. Donga S, Chanda S, 2021. Facile green synthesis of silver nanoparticles using *Mangifera indica* seed aqueous extract and its antimicrobial, antioxidant and cytotoxic potential (3-in-1 system). *Artif Cells Nanomed Biotechnol*, 49(1), 292–302.
4. Jain N, Jain P, Rajput D, Patil UK, 2021b. Green synthesized plant-based silver nanoparticles: Therapeutic prospective for anticancer and antiviral activity. *Micro Nanosyst Lett*, 9(1), 1–24.
5. Seerangaraj V, Sathiyavimal S, Shankar SN, Nandagopal JGT, Balashanmugam P, Al-Misned FA, Pugazhendhi A, 2021. Cytotoxic effects of silver nanoparticles on *Ruellia tuberosa*: Photocatalytic degradation properties against crystal violet and coomassie brilliant blue. *J Environ Chem Eng*, 9(2), 105088.
6. Rengasamy M, Anbalagan K, Kodhaiyolii S, Pugalenthi V, 2016. Castor leaf mediated synthesis of iron nanoparticles for evaluating catalytic effects in

transesterification of castor oil. *RSC Adv*, 6(11), 9261–9269.

7. Sastry M, Mayya KS, Bandyopadhyay K, 1997. pH dependent changes in the optical properties of carboxylic acid derivatized silver colloidal particles. *Colloids Surf A Physicochem Eng Asp*, 127(1–3), 221–228.
8. Bindhu F, Umadevi M, 2013. Surface plasmon resonance optical sensor and antibacterial activities of biosynthesized silver nanoparticles. *Spectrochim Acta A Mol Biomol Spectrosc*, 121C (4), 596–604.
9. Padmini R, Nallal VUM, Razia M, Sivaramakrishnan S, Alodaini HA, Hatamleh AA, Chung WJ, 2022. Cytotoxic effect of silver nanoparticles synthesized from ethanolic extract of *Allium sativum* on A549 lung cancer cell line. *J King Saud Univ Sci*, 34(4), 102001.
10. Jyoti K, Singh A, 2016. Green synthesis of nanostructured silver particles and their catalytic application in dye degradation. *J Genet Eng Biotechnol*, 14(2), 311–317.
11. Mariadoss AVA, Ramachandran V, Shalini V, Agilan B, Franklin JH, Sanjay K, Tawfiq MA, Ernest D, 2019. Green synthesis, characterization and antibacterial activity of silver nanoparticles by *Malus domestica* and its cytotoxic effect on MCF-7 cell line. *Microb Pathog*, 135, 1–9.
12. Vasantharaj S, Sathiyavimal S, Senthilkumar P, Kalpana VN, Rajalakshmi G, Alsehli M, Pugazhendhi A, 2021. Enhanced photocatalytic degradation of water pollutants using bio-green synthesis of zinc oxide nanoparticles (ZnO NPs). *J Environ Chem Eng*, 9(4), 105772.
13. Rajivgandhi GN, Ramachandran G, Kannan MR, Velanganni AAJ, Siddiqi MZ, Alharbi NS, Li WJ, 2022. Photocatalytic degradation and anti-cancer activity of biologically synthesized AgNPs for inhibition of MCF-7 breast cancer cells. *J King Saud Univ Sci*, 34(1), 101725.